JOURNAL OF QUATERNARY SCIENCE (2014) **29**(1) 14–26 ISSN 0267-8179. DOI: 10.1002/jqs.2648

North-eastern Laurentide, western Greenland and southern Innuitian ice stream dynamics during the last glacial cycle

QUENTIN SIMON,[1]* CLAUDE HILLAIRE-MARCEL,[1] GUILLAUME ST-ONGE[1,2] and JOHN T. ANDREWS[3]
[1]GEOTOP-UQAM, Montreal, QC, Canada
[2]Canada Research Chair in Marine Geology, ISMER-UQAR, Rimouski, QC, Canada
[3]INSTAAR, University of Colorado, Boulder, CO, USA

Received 29 October 2012; Revised 22 April 2013; Accepted 12 June 2013

ABSTRACT: Precise relationships between high-frequency ice sheet dynamics and late Quaternary climate variability are still poorly understood, notably with regard to their relative timing and causal mechanisms. Baffin Bay is of particular interest in this regard due to the influence of ice streaming activities from the north-eastern Laurentide, southern Innuitian and western Greenland ice margins on its sedimentary regimes during glacial times. Here we document such ice margin dynamics using a sedimentological analysis performed on a piston core from central Baffin Bay and spanning the last 115 ka. Lithofacies analysis and mineralogical assemblages are used to reconstruct sediment sources (using the SedUnMix program) and depositional mechanisms. Coarse detrital carbonate (DC, dolomite-rich) layers are attributed either to north-eastern Laurentide and Innuitian ice stream surges or to pervasive ice rafted debris delivery processes at distinct periods. Out-of-phase fine-grained glaciomarine sediments with a mineralogical signature from western Greenland, linked to Uummannaq ice streaming activity, are interbedded with the coarse DC layers. The new results suggest that during the last glacial cycle, the north-eastern Laurentide and southern Innuitian ice streams were sensitive to high-frequency climate fluctuations, such as the Dansgaard–Oeschger events, while the western Greenland margins were more sensitive to large-scale climatic/oceanic reorganizations, such as relative sea-level changes and/or advection of warmer Atlantic waters into the bay. Copyright © 2013 John Wiley & Sons, Ltd.

KEYWORDS: Baffin Bay; ice stream; last glacial cycle; sediment provenance; X-ray diffraction.

Introduction

Over the last few decades, ice sheet and glacier dynamics have received considerable attention, notably due to accelerated melting of the Greenland Ice Sheet (GIS) and major outlet retreats (e.g. Weidick and Bennike, 2007; Holland *et al.*, 2008; Alley *et al.*, 2010; Rignot and Mouginot, 2012). Numerous studies and publications have also focused on past ice sheet dynamics, especially with regard to the linkages between Laurentide Ice Sheet (LIS) instabilities and Quaternary climatic changes (e.g. MacAyeal, 1993; Bond and Lotti, 1995; Bond *et al.*, 1999; Dowdeswell *et al.*, 1995, 1997, 1999; Andrews, 2000; Andrews and Maclean 2003; Hemming, 2004; Hulbe *et al.*, 2004). The growth and decay of ice sheets are controlled by (1) mass balance parameters (e.g. accumulation of snow and ice, calving at marine-based margins, basal melting) relating to atmospheric and oceanic changes (Marshall and Koutnik, 2006), and (2) intrinsic ice sheet instabilities (e.g. Heinrich events). The mass balance and stability of ice sheets is associated with rapidly flowing ice streams and outlet glaciers along their margins (Stokes and Clark, 2001). The modeling of the ice sheet responses to past and present climatic changes is a prerequisite to understanding their past behavior and is essential for interpretation of the ongoing ice stream retreats along the Greenland ice margin. Building such simulations requires knowledge of rates and timing of the rapid and/or long-term ice streaming processes (Stokes and Tarasov, 2010). However, the triggering and driving mechanisms behind such processes and their timing are still poorly documented. As a consequence, recent changes in Greenland ice margin dynamics could be attributed to either climate/ocean warming (through mass balance changes) or to longer-term changes in the GIS budget responses to Holocene climate changes (i.e. a mix of mass balance and internal dynamics; Stokes *et al.*, 2012).

In this respect, and because it was surrounded by some of the largest Late Quaternary ice sheets, Baffin Bay holds great interest for the identification of ice margin dynamics [i.e. the western Greenland, north-eastern (NE) Laurentide and southern Innuitian Ice Sheets] from its sedimentary records. To achieve this, the recognition of sedimentary features in terrigenous layers that are characteristic of their origin, transport and depositional mechanisms is required. In addition, the temporal relationship between such layers and high-frequency ice sheet and/or climate variability is also critical. Until now, the interpretations of sedimentary sequences from Baffin Bay have proven challenging due to the lack of well-dated records (Simon *et al.*, 2012). Moreover, very few marine geophysical and geological data reflecting ice stream advances and retreats pre-dating the Last Glacial Maximum (LGM) are available, due largely to ice erosion during the LGM itself and the last deglaciation (Andrews *et al.*, 1998; Alley *et al.*, 2010), thus hampering any direct reconstruction of the longer (pre-LGM) history of paleo-ice streams and their dynamics during glacial times.

In this paper, we use sedimentological and mineralogical properties of a piston core (HU2008-029-016PC, Fig. 1) raised from central Baffin Bay and spanning the last 115 ka (Simon *et al.*, 2012) to document surrounding ice margin dynamics. Lithofacies analysis and mineralogical assemblages are used to unravel and discuss sediment provenance and depositional mechanisms. The main objectives of this paper are to (i) reconstruct sediment provenances based on mineralogical assemblages (using the SedUnMix program developed by Andrews and Eberl, 2012), (ii) compare provenance signatures and transport/depositional processes, (iii) document the advance and retreat of western Greenland and eastern Baffin Island ice margins, and their timing with regard

*Correspondence: Q. Simon, as above.
E-mail: quentin.simon@gmx.com

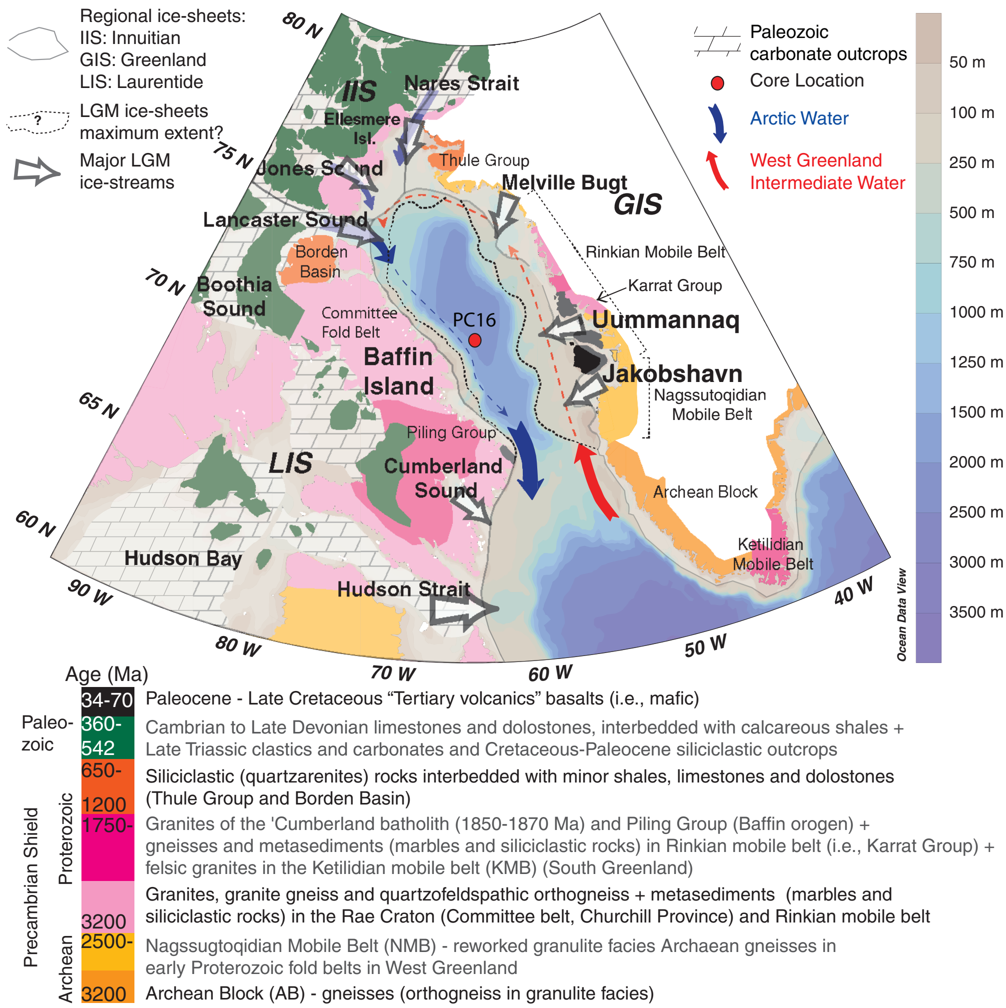

Figure 1. Baffin Bay general map and core location. The bathymetry, oceanic circulation and simplified bedrock geology are from www.geus.dk, Harrison *et al.* (2011) and Tang *et al.* (2004). Last Glacial Maximum limits of the Greenland (GIS), Innuitian (IIS) and Laurentide (LIS) ice sheets and major ice stream locations are adapted from Funder *et al.* (2011), Ó Cofaigh *et al.* (2012, 2013), Dyke (2004), England *et al.* (2006) and Li *et al.* (2011).

to climatic/oceanic variability (e.g. Dansgaard–Oeschger cycles) during the last glacial cycle, and (iv) compare these reconstructions with recent model experiments (e.g. Ganopolski *et al.*, 2010; Stokes *et al.*, 2012).

Regional setting

Baffin Bay (Fig. 1) is a narrow oceanic basin (1300 km long and 450 km wide, ~690 000 km^2) resulting from the extension of the North Atlantic-Labrador Shelf Sea rift system (Maclean *et al.*, 1990). Surface current circulation is counterclockwise in the bay (Tang *et al.*, 2004; Fig. 1). Extensive sea ice (mainly first-year sea ice) covers the bay except in August and September. The influence of Atlantic waters on the Greenland margin contributes to an asymmetric distribution of the sea ice cover (Tang *et al.*, 2004). The present-day fast-flowing outlets of the GIS are estimated to have a total iceberg flux of ~141 km^3 a^{-1} (Bigg and Wadley, 2001), while the contribution from tidewater glaciers on the Canadian Arctic Archipelago are minor (Weidick and Bennike, 2007). Marshall and Koutnik (2006) have estimated the total iceberg flux originating from ice sheets that surrounded Baffin Bay during the last glacial cycle to be ~16.8 × 10^6 km^3.

The bedrock geology of the circum-Baffin Bay region is largely characterized by a Precambrian crystalline basement overlain by a Lower Paleozoic succession dominated by shallow-marine platform carbonates at the northern end of the bay (Hiscott *et al.*, 1989). Paleocene rifting resulted in basaltic flows observed on the Greenland Precambrian Shield margins near the Disko Island and Uummannaq fjord regions (see Fig. 1 for a geological overview, and Harrison *et al.*, 2011, for a detailed geological map of the area). Baffin Bay is bounded to the north by Nares Strait, a probable transform fault, and to the south by the Ungava transform fault system underlying Davis Strait (Ehrhardt *et al.*, 2008). The central abyssal plain (2000–2500 m) is surrounded by steep continental slopes on both sides, while the northern slope dips slightly towards the abyssal plain (Li *et al.*, 2011). Thick sedimentary strata are found along the narrow east Baffin Island shelf (25–50 km) and the opposing and much broader west Greenland shelf (>250 km), which is also characterized by large submarine fans at the mouth of cross-shelf troughs (Jakobsson *et al.*, 2012).

The identification and recent interpretation of a series of major submarine fans located at the mouths of western Greenland cross-shelf troughs (e.g. Uummannaq fan at the mouth of the Uummannaq Trough), and marine geophysical and geological data provide clear evidence for a former extension of fast-flowing grounded ice streams across the West Greenland continental shelf during the LGM (Ó Cofaigh *et al.*, 2012, 2013). Such major fan structures are either absent or very limited on the narrower eastern Baffin Island shelf. Ó Cofaigh *et al.* (2012) suggested that these geomorphological discrepancies may be explained by the wider Greenland shelf together with larger ice sheet outlets, as these allow a large ice stream flow path on the Greenland side, while the shorter continental shelf and smaller fjord outlets from Baffin Island do not favor the development of large ice streams. Furthermore, the repeated occupation of major cross-shelf troughs by successive grounded ice streams during glacial maxima has probably increased the erosion and recycling of Greenland shelf sediments and their delivery offshore into Baffin Bay.

Glacial history

During the LGM, the NE LIS, the Innuitian Ice Sheet (IIS) and the western GIS constituted an almost continuous ice belt surrounding Baffin Bay (Fig. 1). NE LIS and southern IIS ice streams (in Lancaster Sound, Jones Sound and Smith Sound – Nares Strait) advanced into northern Baffin Bay (MacLean *et al.*, 2010) with an LGM grounding line situated 270 km off the mouth of Lancaster Sound (in a water depth of 1300 m; Li *et al.*, 2011) and potentially expanded laterally to create an ice shelf in the northern part of the bay (Hulbe *et al.*, 2004; Marcott *et al.*, 2011). The LIS outlets extended through Baffin Island, probably as far as the fjord mouths and inlets, and possibly over part of the Baffin Island shelf (Briner *et al.*, 2003, 2006, 2007; Young *et al.*, 2012), while the GIS outlets expanded westward onto the Greenland inner shelf, and as far as the shelf edge off Disko Bugt and the Uummannaq Trough at the LGM (Ó Cofaigh *et al.*, 2012, 2013). The buildup of the IIS as late as ~19k cal a BP is out of phase with the buildup of the LIS (Dyke *et al.*, 2002; England *et al.*, 2006, 2009), which had attained its maximum extent between 24 and 20k cal a BP, while the GIS margin was probably close to its maximum extent as late as ~15k cal a BP (Funder *et al.*, 2011; Ó Cofaigh *et al.*, 2013). This phasing and the continued fall of global eustatic sea level until ~18k cal a BP indicate that growth of the LIS, GIS and IIS probably responded to different forcings (Clark and Mix, 2002; Dyke *et al.*, 2002; England *et al.*, 2006).

Although pre-LGM glaciations are poorly documented around Baffin Bay, the recognition and interpretation of large Baffin Bay Detrital Carbonate (BBDC) layers [i.e. coarse dolomite-rich ice-rafted debris (IRD) layers] in deep Baffin Bay cores (Aksu and Piper, 1987; Andrews *et al.*, 1998, 2013; Parnell *et al.*, 2007) and their precise timing in core PC16 (Simon *et al.*, 2012; Table 1; Figs 2 and 6) confirmed recent numerical simulations (Ganopolski *et al.*, 2010; Stokes *et al.*, 2012) of a rapid NE LIS and IIS inception and extension after the last Interglacial [i.e. Marine Isotope Stage (MIS)5e], followed by several phases of ice sheet growth and reduction during the last glacial cycle. Simon (2013) suggested two causal processes to explain the deposition of BBDC layers: (i) the initiation and extension of fast-flowing ice streams from the northern end of Baffin Bay (i.e. especially from the large Lancaster Sound ice stream) with increasing iceberg flux over a long period; and/or (ii) a rapid destabilization of the sea-ice/ice shelf covering Baffin Bay, which would trigger northern ice streams (i.e. Lancaster and Jones Sound) surges producing deposition of BBDC layers over short periods. These causal processes were probably related to external forcing, such as the Dansgaard–Oeschger cycles (i.e. mass balance factors), rather to internal ice sheet instabilities (i.e. ice sheet dynamics processes and associated surges) (Marcott *et al.*, 2011; Petersen *et al.*, 2013).

Table 1. Timing and duration of the Baffin Bay Detrital Carbonate layers (BBDC).

BBDC layers*	BBDC timing interval (cal ka BP)	BBDC duration (ka)
	10.5–12	1.5
1	13.7–15	1.3
2	24.7–25	0.3
3	26.4–27.7	1.3
4	31.9–37	5.1
5	48.5–50	1.5
6	58–64	6
7a	73–79.5	6.5
7b	80.5–84.5	4
8a	91.5–95	3.5
8b	99–100.5	1.5
8c	103–104.5	1.5
9a	107.5–108.5	1
9b	110–115?	>5?

*Numbering according to Simon (2013).

Materials and methods

The HU2008-029-016PC piston core, hereafter PC16, is a 741-cm-long piston core raised from central Baffin Bay during the 2008-029 CCGS Hudson expedition (70°46.14′N/64°65.77′W; water depth: 2063 m; Campbell and de Vernal, 2009). The core location (Fig. 1) is near an Ocean Drilling Program (ODP) site that was drilled in 1985 (ODP 645, Leg 105; Srivastava, 1989) and several cores retrieved from the deep central Baffin Bay during the 1970s and 1980s (e.g. Aksu, 1981; Aksu and Piper, 1987; Hillaire-Marcel *et al.*, 1989; Andrews *et al.*, 1998).

Physical and geochemical properties

The core sections (1.5 m long) were described and sampled with u-channels (rigid u-shaped plastic liners, 2×2 cm cross-section) from the center of the working halves. To allow visualization of the sedimentary structures, the archive halves were run through a computerized coaxial tomography (CT) scanner at 1-mm intervals at INRS-ETE in Quebec City (Fig. 2). The results of this scan mainly reflect changes in bulk density (quantified through the CT numbers; e.g. St-Onge *et al.*, 2007). High-resolution micro X-ray fluorescence (μXRF) spectrometry measurements were performed at 0.5-cm intervals and during a 50-s counting time using an ITRAX core scanner (Cox Analytical Systems, Mölndal, Sweden) at the GIRAS (Geochemistry, Imagery and Radiography of Sediment) laboratory of INRS-ETE. The output data represent relative concentrations, which have been reported here as cumulative concentrations (relative to depth) to provide independent information about sedimentation deposition variability (Fig. 2). Grain size analyses were performed on sediment samples (1–2 g) at the Institut des sciences de la mer de Rimouski (ISMER) using a Beckman Coulter LS13320 laser diffraction grain size analyser at 4-cm intervals (Simon *et al.*, 2012).

Mineralogy and SedUnMix

Bulk mineralogical assemblages were determined by X-ray diffraction (XRD) at UQAM using a Siemens D-5000 diffractometer (°2Θ, CoKα1,2 radiation and a silicon detector). Semi-quantitative estimates ($\pm 1\sigma \sim 5\%$) of the main mineral species were based on the peak height (in counts per second) of the first diffraction peak for each mineral corrected for quartz and normalized to 100% (following the method presented by Thorez, 2003). The analyses were performed on sediment fractions sieved at 63 μm and 2 mm with a 4-cm sample interval and then merged to compare our mineralogical assemblages with the source signatures (Andrews and Eberl, 2011). Additional samples were measured to obtain high-resolution results of the mineralogical composition changes where lithofacies variability occurred within the 4-cm interval. We used weighting factors (ratio between the

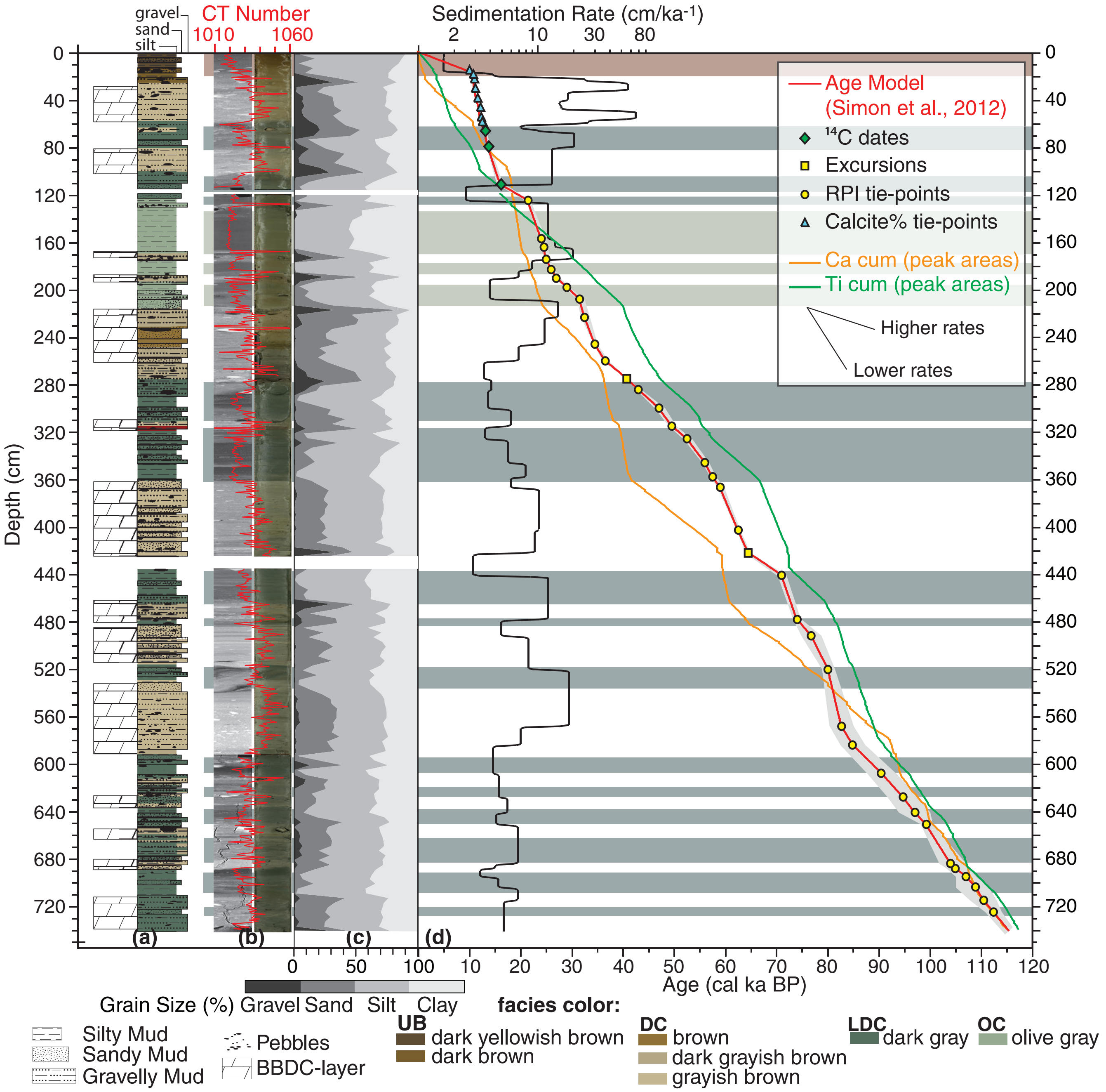

Figure 2. Core PC16 lithostratigraphy and age model. (a) Simplified stratigraphy log (see legend for details). (b) CAT scan image (X-ray) of the core (left) and associated *CT* number (density proxy). High-resolution digital image (right). (c) Grain size distribution (%) for clay (0–2 μm), silt (2–63 μm), sand (63 μm to 2 mm) and gravel (>2 mm). (d) Core PC16 age model (red curve; Simon *et al.*, 2012) and associated sediment accumulation rates. The Ti (green) and Ca (orange) cumulative curves represent the cumulative addition of titanium and calcium relative concentrations (peak areas measured with the μXRF ITRAX core scanner). Gradient changes give independent information about sedimentary depositional process variability. Distinct lithofacies are highlighted with color banding (see text for details).

weight of individual fractions) on both fractions (i.e. <63 and 63 μm to 2 mm) to respect grain-size proportion. High correlation coefficients between the weight percentage and laser grain size analysis ($r = 0.88$ for silt and $r = 0.91$ for sand) confirmed the reliability of the merging process.

To unravel sediment provenance based on the mineralogical composition, we applied the sediment unmixing model (SedUnMix) proposed by Andrews and Eberl (2012). The model calculates the contribution of different source areas of mixed sediments. SedUnMix seeks an iterative solution (we used 20 iterations in this study) to optimize a non-linear solution for the respective percentages of source regions and sample compositions. This iteration process reduces the average absolute difference between the observed and the calculated mineralogy (see Andrews and Eberl, 2012, for details about the method). We ran SedUnMix using data from our new mineralogical semi-quantitative estimates from PC16 and from the different possible sources previously determined by Andrews and Eberl (2011) based on cluster analysis on principal component scores calculated on box cores and surface sediments from across the bay. These possible end-members represent sediment signatures from the Jakobshavn Trough, Uummannaq Trough, eastern Baffin Island and northern Baffin Bay (see Table 4 in Andrews and Eberl, 2011;

and Fig. 1). We decided to exclude the Jakobshavn source in our calculations because (i) our semi-quantitative XRD approach does not yield a detailed record of the feldspar mineral suite, in comparison with the quantitative XRD (qXRD) approach used by Andrews and Eberl (2011), which could induce biases in the provenance calculation (notably precluding a strong distinction between eastern Baffin Island and Jakobshavn signatures). Moreover, (ii) the core location lies off the Uummannaq Trough and too far north of the Jakobshavn Trough outlet to allow for the large presence of Jakobshavn sediments at the study site, as demonstrated by Andrews and Eberl (2011) with analysis of a nearby box core (JCR175-BC06) analysis.

Chronology

The age model of core PC16 (Fig. 2) is based primarily on the correlation of its relative paleointensity (RPI) profile with regional and global RPI reference curves (Simon *et al.*, 2012). Three radiocarbon ages and two geomagnetic excursions further support the established age model. The derived age model is consistent with previous regional age models (de Vernal *et al.*, 1987; Andrews *et al.*, 1998) but offers a much more precise and accurate temporal resolution (see Simon *et al.*, 2012 for details).

Results

Lithofacies

Four major lithofacies were identified and described in the core (Simon *et al.*, 2012). They represent distinctive sediment delivery processes and probable provenance changes during the last glacial cycle and the Holocene (Fig. 2). Olive gray to dark gray poorly sorted sandy muds to slightly gravelly sandy muds with low detrital carbonate percentages [Low Detrital Carbonate (LDC) facies] and carbonate-rich (mainly dolomite) yellowish-brown to dark brown very poorly sorted gravelly sandy muds (corresponding to the BBDC layers) describe mainly the bulk of the core (these two lithofacies are highlighted with white and dark green banding in Fig. 2). Two additional lithofacies are found at specific intervals: the top of the core (0–20 cm) is characterized by brown to dark brown silty muds (Uppermost Brown unit, UB) while the interval between 120 and 215 cm is characterized by brownish-black and olive-black silty muds to clayey muds (Olive clay unit, OC). The UB and OC facies represent sediments deposited solely during the Holocene and an extended MIS2 (16–32 ka), respectively, and characterize specific environmental conditions during these time periods (see Simon *et al.*, 2012, for additional information on the lithofacies and their environmental interpretations).

Mineralogical results

Following this lithofacies interpretation, the XRD relative mineralogical composition demonstrates a significant down-core variability (Fig. 3). Two principal modes are distinguished: (i) carbonate-rich layers with about 30–40% dolomite and 10–15% calcite; and (ii) feldspar-rich layers (i.e. K-feldspar and plagioclase minerals) with values between 30 and 50% associated with increases of clay minerals (Fig. 3). This pattern is consistent with the identification and interpretation of BBDC layers related to the glacial erosion of basement rocks at the northern end of Baffin Bay, where major ice streams of the NE LIS and north-western GIS merged (Aksu and Piper, 1987; Andrews *et al.*, 1998; Parnell *et al.*, 2007). Feldspar-rich layers are probably associated with lateral sources (from Greenland and Baffin Island), while the feldspar minerals are highly diluted by more rapid erosion of carbonate rocks at the northern end of the bay (Parnell *et al.*, 2007; Andrews and Eberl, 2011). Coarse sediments characterize the carbonate-rich layers, while the LDC facies is accompanied by an increase in the clay and silt fractions (Fig. 3). The content of clay minerals, especially illite, increases in the LDC, UB and OC facies (Fig. 3). The large increase of smectite relative content in the OC facies is probably associated with the erosion of the Tertiary basalt terrains from the Uummannaq region (Figs. 1 and 3; Simon, 2013).

SedUnMix tuning

To test the reliability of our semi-quantitative estimate with the qXRD method used by Andrews and Eberl (2011) for source identification, we measured ten samples with the qXRD method described in Eberl (2003, 2004). The results present nearly identical relative distribution and similar percentage values (within the statistical uncertainty, Supporting information, Fig. S1). Nevertheless, a large deviation of the quartz weight percentage in one sample, associated with the overall ubiquity of quartz in the source composition (12.7 ± 7.2 wt%), raised the question of its impact on the provenance calculation. We therefore ran SedUnMix analyses (ten iterations) by including/excluding the quartz. The results without the quartz have lower degrees-of-fit (DOF, 0.42 ± 0.21 vs. 0.56 ± 0.31) and smaller average deviation values (a measure of the level of agreement between the observed and expected mineralogy, 2.37 ± 1.38 vs. 3.12 ± 1.66), thereby expressing a better fit between sources and core samples (Andrews and Eberl, 2012). Accordingly, we removed the quartz from the mineralogical assemblage to improve the geographical clustering and avoid misinterpretation of some results caused by methodological differences between sources and down-core sample measurements. Besides, the dissolution of carbonates in deep-basin surface sediments (due to corrosive waters, see Azetsu-Scott *et al.*, 2010) introduces an important 'no analog' problem, as the mineralogical assemblage failed to accurately represent the respective sources with respect to the carbonate contents as previously demonstrated by Andrews and Eberl (2011). Consequently, the carbonate minerals have also been removed from the mineralogical assemblage. The removal of dolomite, calcite and quartz from the mineralogical assemblage reduced the possibility of misinterpreting the provenance calculation results using our semi-quantitative estimates (based on the partial composition using the eight mineralogical species selected, which have been summed to 100%) and the SedUnMix program. An important consequence of the removal of the carbonates implies that the weight percentages calculated between the sources are relative and not absolute due to the artificial reduction of the northern Baffin Bay contribution. Then, weight percentages represent lateral source contributions (i.e. eastern Baffin Island versus western Greenland, Fig. 4), while the BBDC signal is significantly reduced. This is of particular interest for reconstructing the lateral source changes and their precise timing, as the strong BBDC signal may prevent the recognition of these changes. Consequently, we interpret our results in terms of relative change in any given source activity (ice stream dynamics) in time rather than providing a precise estimate of sediment provenance.

Finally, we compared the results of SedUnMix runs on ten samples measured with the semi-quantitative and qXRD methods. For the last glacial period, the results yield comparable source contributions, with high correlation

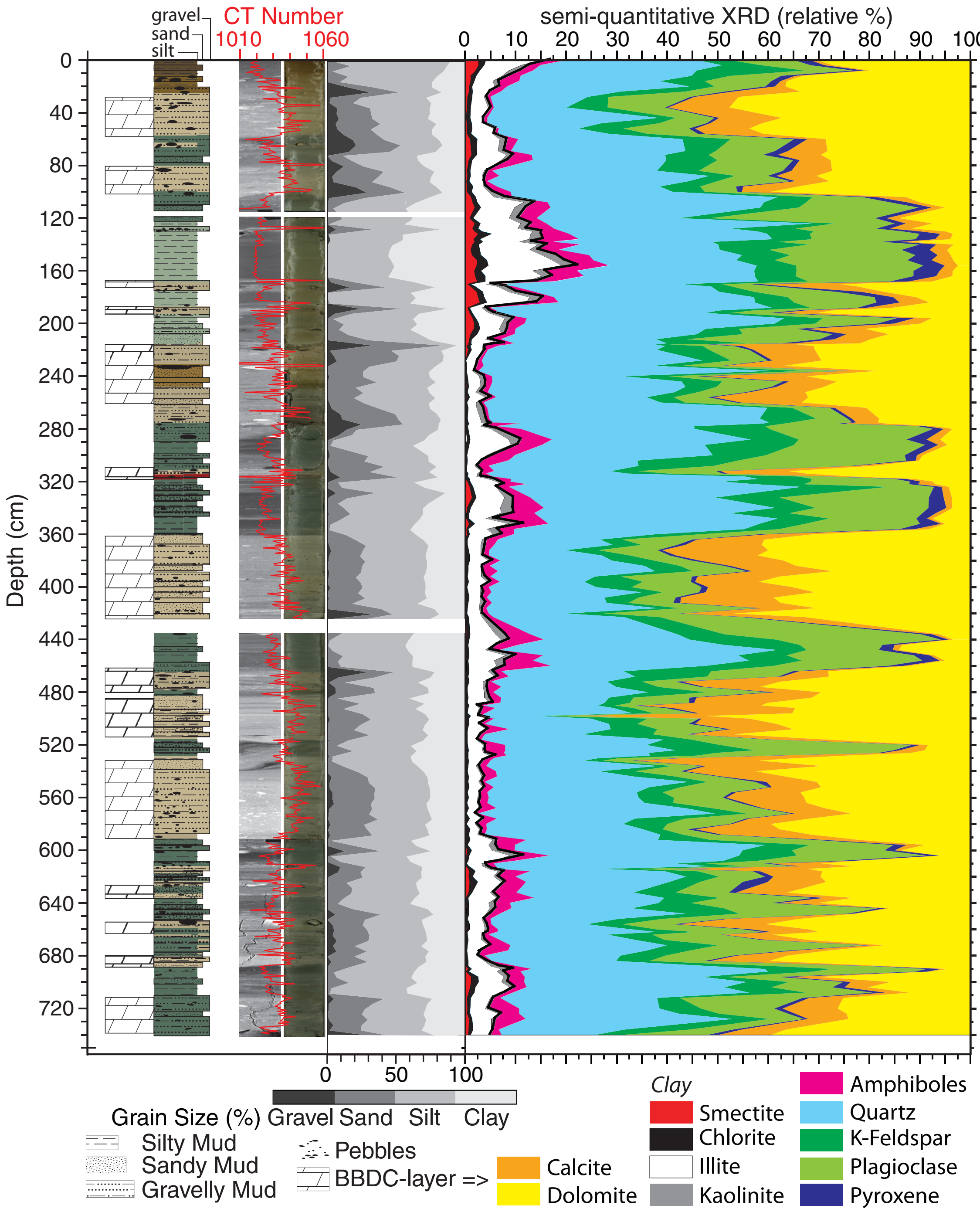

Figure 3. Core PC16 relative XRD mineralogical assemblages (calculated on the most abundant minerals and summed to 100%). This figure is available in colour online at wileyonlinelibrary.com.

coefficients for Uummannaq ($r = 0.90$) and eastern Baffin Island ($r = 0.85$) (supporting Fig. S2), which validate the use of semi-quantitative estimates for the provenance calculation using SedUnMix.

Provenance changes

Given the distinct lithofacies already described and the mineralogical composition variability, we expect to find variations in sediment provenance within the core. This is well illustrated by comparing the composition of the surface samples (i.e. the top two samples) with the down-core assemblages using a SedUnMix calculation. Large deviations from 100% are observed within several layers, indicating major changes in primary sediment sources throughout the core (up to 40 wt%, Fig. 4). The larger deviations appear mainly within the BBDC layers, corresponding probably with major changes in the transport process (i.e. ice rafting) between these intervals and modern sedimentation settings.

According to our analysis, the largest non-carbonate and non-quartz contribution is attributed to Uummannaq (average 53.7 wt%) and eastern Baffin Island (38.5 wt%) sources, while the northern Baffin Bay source is nearly absent from the calculation (0.5 wt%) (Fig. 4). The fraction of source not resolved by the program is relatively low (7.3 wt%). These values confirm the removal of the BBDC signal (i.e. northern Baffin Bay sources) from the calculation. A very large increase

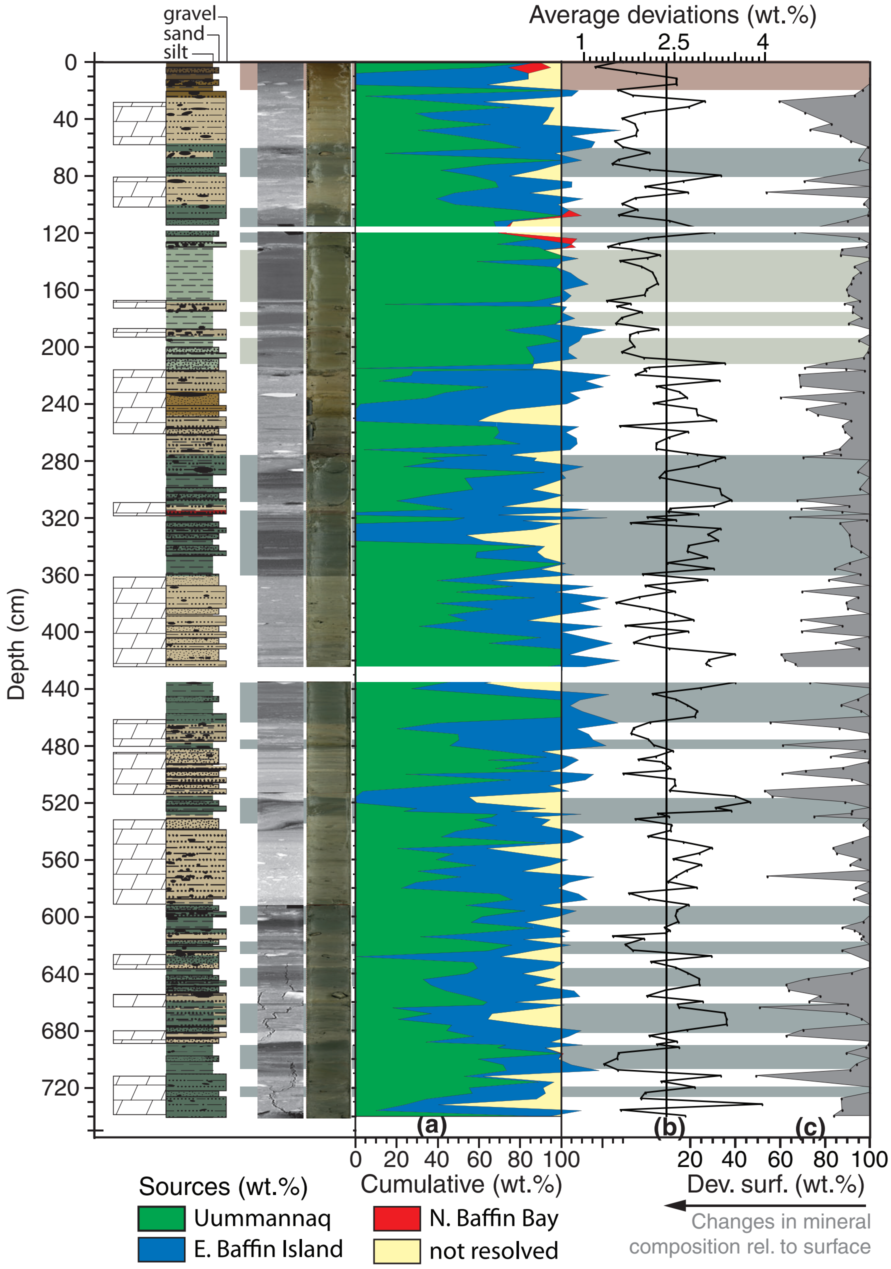

Figure 4. (a) Cumulative wt% contributions from the three major sediment sources (Uummannaq, east Baffin Island and northern Baffin Bay) calculated from the mineralogical assemblages using SedUnMix (Andrews and Eberl, 2012). 'Not resolved' indicates that the sum wt% was < 100%. (b) Average wt% species deviations for each sample based on three sources and excluding carbonate (dolomite + calcite) and quartz. (c) Mineralogical-assemblage deviation (wt%) between surface and downcore samples. Large deviations from 100% indicate major changes in mineral composition. This figure is available in colour online at wileyonlinelibrary.com.

of nearly 100 wt% of the Uummannaq sediments corresponds to the facies OC (Fig. 4), while a 2nd peak of nearly 100 wt% is found between 410 and 460 cm. These peaks correspond to major sediment deliveries from Greenland, probably corresponding to important GIS ice margin advances while several peaks of Uummannaq sediments (>60 wt%) probably relate to reduced ice margin extensions on the Uummannaq Trough. Several peaks of sediments from eastern Baffin Island (>50 wt%) are observed episodically through the core while the higher values, comprising between 60 and 80 wt%, characterized the interval 215–255 cm (Fig. 4). The larger eastern Baffin Island wt% values are mainly found within the coarser carbonate-rich BBDC intervals.

Principal component analysis

Principal components analysis (PCA) was used to simplify the dataset to only a few primary clusters that retain the main features of the mineralogical and grain-size variability (Davis, 2002). The first two principal components accounted for 52% (PC1 40.7% and PC2 11.3%) of the total variance (Fig. 5). PC1 has positive loadings for finer sediments, such as clay and very fine silts (i.e. 'glacial flour'; Table 2). These positive loadings with the Uummannaq source are coherent with the hypothesis of fine-grained sediments originating from Greenland ice streams (Fig. 6). By contrast, PC1 has negative loadings with proxies of coarse detrital carbonate layers, such as XRD dolomite and calcite, chlorite, CT number (density) and sand (Table 2). Therefore, positive loadings on PC1 probably represent western Greenland ice margin advance stages, while negative loadings on PC1 are associated with coarser sediments originating from either eastern Baffin Island or the northern end of the Baffin Bay. Given this association between mineralogy and grain size, the mineralogical variability is probably a combination of changes in sediment delivery processes at the ice margin and sediment transport (i.e. shown by grain size variability), as well as of sediment provenance. Minerals in the upper right quadrant could come from either eastern Baffin Island or Greenland crystalline rocks, whereas minerals in the lower left quadrant are related to the northern Paleozoic carbonate outcrops.

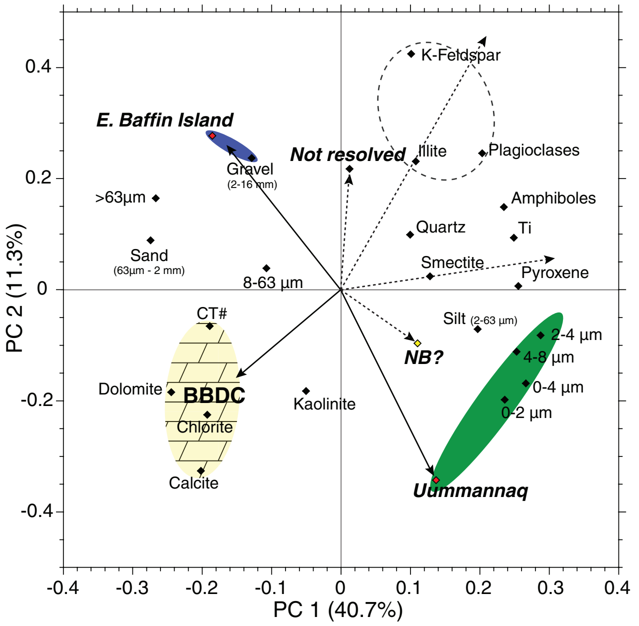

Figure 5. Principal component analysis (PCA) of the mineralogical and grain-size dataset. The loading scores for PC1 vs. PC2 explain, respectively, 40.7 and 11.3% of the total variance. PCA analysis illustrates the two sedimentary modes in Baffin Bay during the last glacial cycle. The colored ellipses represent sediments signatures from the three main sources discussed (using the same color as in Figs. 4 and 6). This figure is available in colour online at wileyonlinelibrary.com.

Discussion

In contrast to the coarse dolomite-rich IRD layers (i.e. BBDC) released from northern ice streams, fine-grained Ti-rich sediments in the LDC facies have been related to a 'lateral' mode characterized by sediment supplies from the advances and/or retreats of western Greenland and eastern Baffin Island ice streams (Aksu and Piper, 1987; Hiscott *et al.*, 1989). However, to date no common provenance proxies have confirmed such a 'lateral' source provenance or provided a means to distinguish and quantify between sediment originating from eastern Baffin Island or western Greenland. In this study, the removal of carbonates (dolomite and calcite) from the mineralogical composition allows us to eliminate the strong BBDC imprint, thereby highlighting the variability of sediments from the 'lateral' sources (Figs. 4 and 6) and reducing the intermingling impact of Greenland and Laurentide supplies. These new results illustrate a clear distinction between western Greenland and eastern Baffin Island sediment supplies, confirming the usefulness of the mineralogical approach (Fig. 4). The new data also reveal distinct deposition patterns, with sharp peaks of eastern Baffin Island coarse sediments that are interbedded with more steady supplies of Uummannaq fine-grained sediment (Fig. 6). These observations raised two questions: (i) Were the lateral ice streams from western Greenland and Baffin Island in phase and/or did they relate to distinct processes? (ii) Were these lateral ice stream advance/retreat phases driven by climatic and/or oceanic reorganization processes (i.e. mass balance) similar to northern ice streaming pulses or rather related to ice sheet dynamics (i.e. ice sheet surges)?

Eastern Baffin Island

The larger eastern Baffin Island sediment pulses (>50 wt%) correspond typically to short intervals (<1 ka) occurring within the BBDC layers (Fig. 4), pointing to a similar activating mechanism and deposition processes. The correspondence of sediment delivery between these sources suggests synchronous dynamics from separated ice streams located over the Canadian Arctic Archipelago and Baffin Island. This apparent synchronicity suggests that climate/

Table 2. Principal component analysis (PCA) data and Pearson correlation coefficients.

Loading	PC1	PC2	PC3	PC1	PC2
Eigenvalues	10.57	2.94	2.6		
Variance (%)	40.68	11.34	9.99		
Variance (cumulative %)	40.68	52.02	62.01		
	–	–	–	*r*	*r*
Quartz	0.10	0.10	0.34	0.32	0.17
K-feldspar	0.10	0.42	0.03	0.33	0.73
Plagioclase	0.20	0.25	–0.03	0.66	0.42
Amphibole	0.23	0.15	–0.08	0.76	0.26
Pyroxene	0.26	0.01	0.04	0.83	0.01
Calcite	–0.20	–0.33	–0.16	–0.66	–0.56
Dolomite	–0.24	–0.18	–0.16	–0.79	–0.32
Smectite	0.13	0.02	0.34	0.42	0.04
Illite	0.11	0.23	–0.46	0.35	0.40
Kaolinite	–0.05	–0.18	0.46	–0.16	–0.31
Chlorite	–0.19	–0.23	0.18	–0.63	–0.39
Gravel%	–0.13	0.24	–0.05	–0.42	0.41
Sand%	–0.27	0.09	0.06	–0.89	0.15
>63 µm (%)	–0.27	0.16	0.03	–0.87	0.28
Silt (0–63 µm) (%)	0.20	–0.07	0.18	0.64	–0.12
Clay (0–2 µm) (%)	0.24	–0.20	–0.23	0.77	–0.34
Very fine silts (2–4 µm) (%)	0.29	–0.08	0.00	0.94	–0.14
'Glacial flour' (0–4 µm) (%)	0.27	–0.17	–0.17	0.87	–0.29
Medium to coarse silt (8–63 µm) (%)	–0.11	0.04	0.24	–0.35	0.07
C_T no. (density)	–0.19	–0.07	–0.14	–0.61	–0.11
Ti (peak area)	0.25	0.09	0.14	0.81	0.16
Uummannaq wt%	0.14	–0.34	–0.07	0.45	–0.59
Eastern Baffin Island wt%	–0.19	0.28	0.05	–0.60	0.48
Northern Baffin Bay wt%	0.11	–0.10	0.13	0.36	–0.17
Not resolved wt%	0.01	0.22	0.04	0.04	0.37

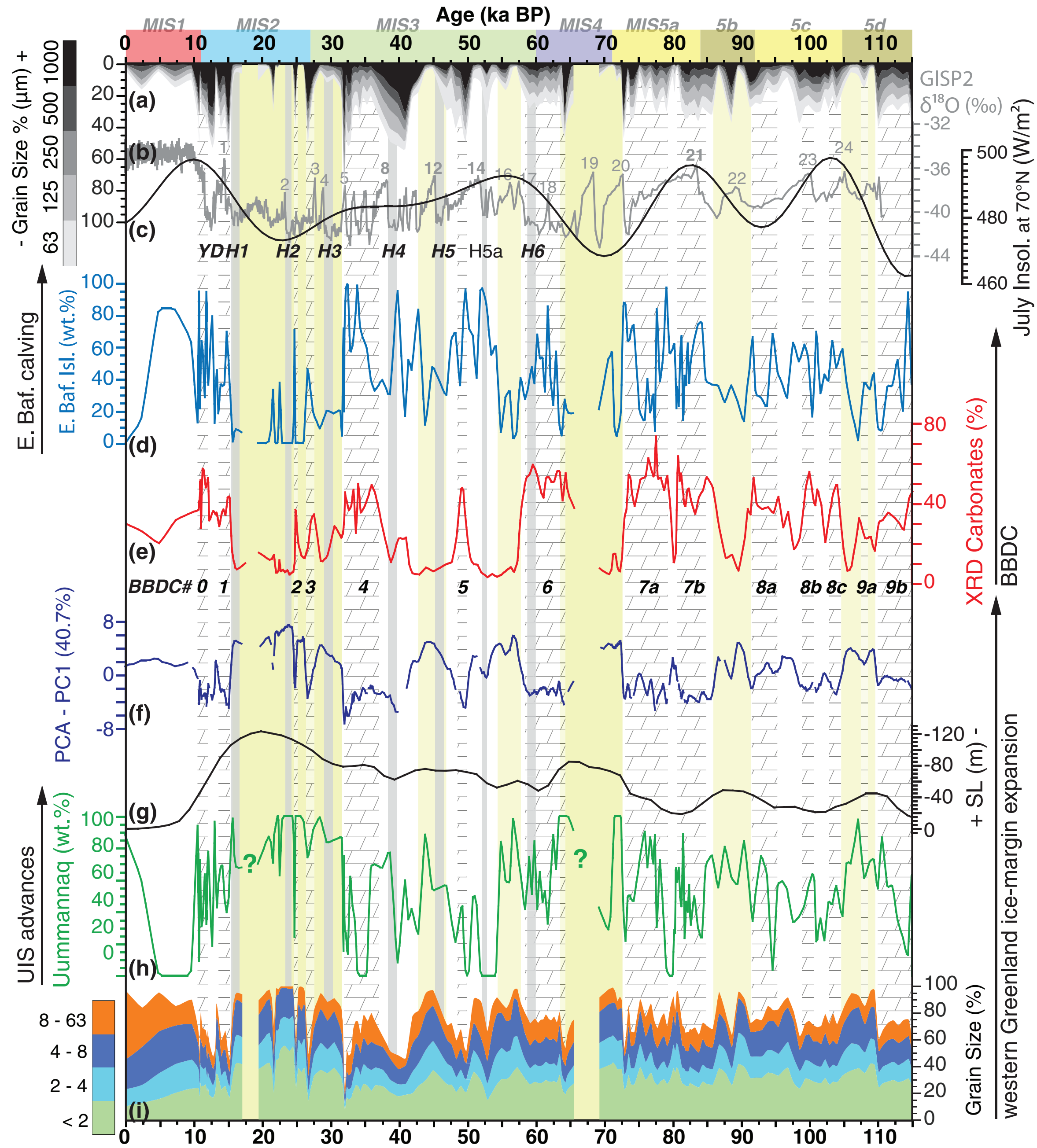

Figure 6. Sediment provenance and grain-size variability during the last glacial cycle. (a) Coarse grain size distribution (%) per size fraction (see legend). (b) GISP2 $\delta^{18}O$ and Greenland interstadials (1-24). (c) July insolation values calculated at the site latitude (Laskar *et al.*, 2004). (d) Eastern Baffin Island wt% contribution. (e) XRD carbonate (dolomite + calcite) relative percentages. (f) First component (40.7%) of the PCA analysis. (g) Sea level record (SL, *y*-axis reverse) from Waelbroeck *et al.* (2002). (h) Uummannaq ice stream (UIS) wt% contribution. Large increases of Uummannaq sediments are highlighted by green banding. (i) Grain-size distribution (%) of clay and silt fractions. Marine isotopic stages (MIS1 to MIS5d) are represented by color boxes along the age axis. Baffin Bay Detrital Carbonate (BBDC) layers are represented by a vertical brick pattern and numbered according to Simon *et al.* (Simon, 2013; see Table 1). Heinrich events are represented by gray lines according to Hemming (2004).

ocean played a significant part in the ice dynamics of these regions. The timing of these sharp peaks of eastern Baffin Island sediments corresponds to Dansgaard–Oeschger events (Greenland interstadials recorded by higher $\delta^{18}O$ values in the GISP2 ice core, Fig. 6), except for a large peak at the end of MIS5a (associated with a fast-flowing northern Baffin Bay ice stream episode, explaining the deposition of the BBDC-7a layer, Simon, 2013). Therefore, the eastern Baffin Island ice margin dynamics was probably driven by external parameters, such as Dansgaard–Oeschger cycles, rather than internal ice sheet processes.

Hence, we suggest that the contribution of eastern Baffin Island sediments to the central Baffin Bay sedimentary budget (at least at the core location, Fig. 1) would correspond to the release of IRD and meltwater plumes from the calving and melting of marine-based glacier outlets, or of grounded ice streams that advanced onto the outer fjords area. During intervals of glacial retreat and/or fast flowing ice streams (Simon, 2013), an IRD sedimentary setting would resume in Baffin Bay with the deposition of BBDC layers, linked to northern sources as indicated by the presence of large amounts of dolomite-rich carbonates as well as to pulses of coarse sediments from the eastern Baffin Island margin (Fig. 6). These coarse IRD horizons were probably deposited during periods when ice margins retreated behind their maximum extent following oceanic circulation increase and subsurface warming in the bay (Fig. 7a). During such episodes, western Greenland sediments would have been

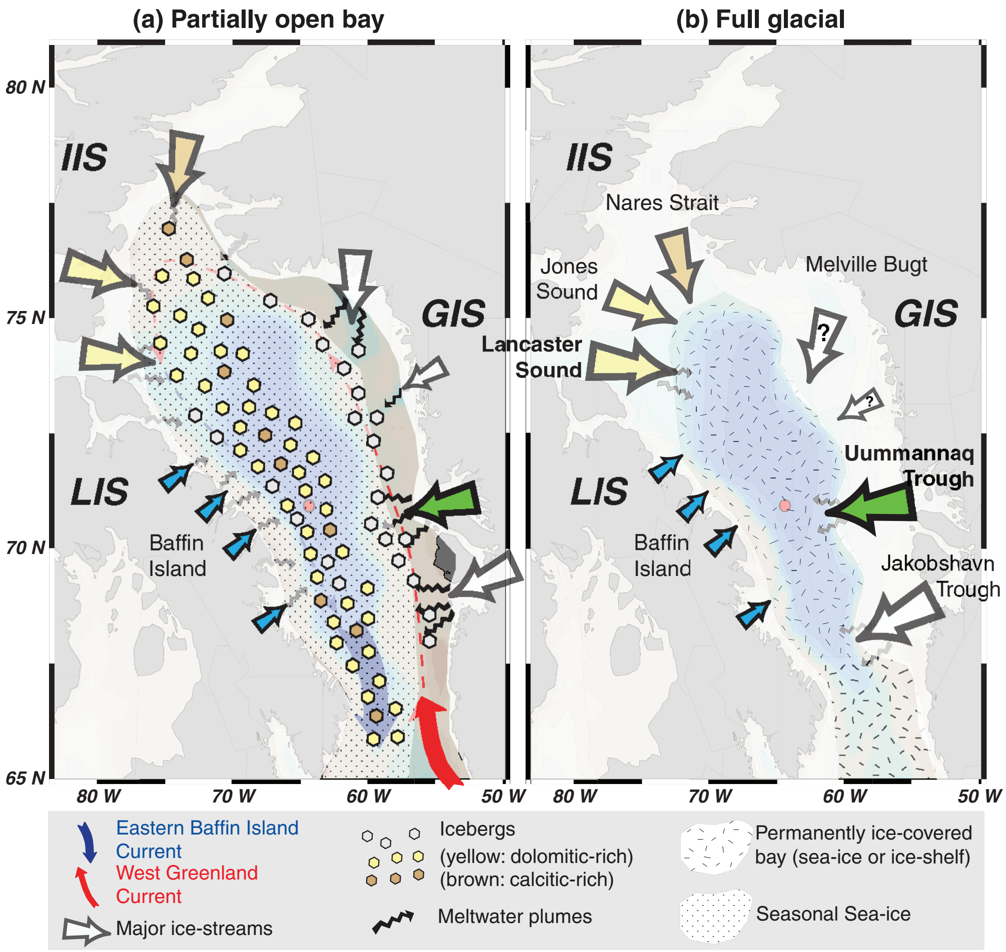

Figure 7. Simplified Baffin Bay paleogeography during the last glacial cycle. (a) Partially open bay characterized by IRD sediments originating from the northern ice streams, and by meltwater plumes from Baffin Island ice streams. (b) Full glacial mode characterized by Greenland and Baffin Island glacial flour sediments corresponding to a permanently ice-covered bay, and by extended fast-flowing ice streams (i.e. Lancaster and Uummannaq) probably feeding an ice shelf in the bay.

mostly deposited over the Greenland shelf rather than being transported farther away towards the center of the bay (Fig. 7a), while iceberg circulation and melting delivered northern and western sediments to central Baffin Bay.

Western Greenland (Uummannaq)

Interbedded with the rapidly deposited coarse sediments from northern and western Baffin Bay, the large increases in Uummannaq-sourced, fine-grained sediments are interpreted as indicating a stable and relatively long-duration (>5 ka) Greenland ice sheet expansion and development, notably over the Greenland shelf along Uummannaq Trough. Large increases in Uummannaq sediment deliveries (i.e. > 60 wt%) occurred within the intervals 110–105, 91–85, 72–63 and 32–16 ka, while two additional smaller Uummannaq weight percentage peaks are found between 58 and 55 ka and around 44 ka (Fig. 6). From these results, we suggest that the Uummannaq Trough ice stream expanded over the Greenland shelf immediately after the onset of the northern glacial inception after the last Interglacial (as early as 110 ka) and was followed by subsequent advances during colder episodes (highlighted by green banding in Fig. 6). Two of these advances are characterized by wt% values of nearly 100% and large peaks of glacial flour (Figs 5 and 6). They occurred during an 'extended MIS2' interval (32–16 ka) and during MIS4 (72–63 ka). The smaller ones (i.e. 80 wt%) correspond to MIS5b (91–85 ka) and late MIS5d (110–105 ka) intervals, respectively (Fig. 6). The large fast-flowing ice streams over the large Greenland cross-shelf troughs have probably contributed to increase Greenland sediment erosion and sediment delivery rates into Baffin Bay, while smaller ice stream systems from Baffin Island did not permit high sediment loads to be deposited at the core location during glacial maxima.

The recording of nearly 100% of Uummannaq sediments during the LGM confirms the development of a grounded, fast-flowing ice stream in the Uummannaq Trough as far as the shelf edge that delivered glaciomarine sediments to the Uummannaq fan and into deep central Baffin Bay, as recently proposed by Ó Cofaigh *et al.* (2012, 2013). The observed mineralogical signatures in our site indicate large Uummannaq ice stream extent and/or activity from ~32 to nearly 16 ka (Fig. 6). Therefore, from our study, we propose that the last massive growth of the western GIS (reaching a maximum extent during the LGM, *sensu stricto*) started from ~32 ka, while substantial ice stream retreat from the Greenland shelf did not begin before ~16k cal a BP (Fig. 6).

The other Uummannaq sediment pulses (e.g. MIS5d and 5b, MIS4) probably corresponded to somewhat reduced advances and thickenings of the GIS outlet glaciers on the Greenland shelf. The very high percentages of Uummannaq sediments (almost 100%) and a fine grain size signature (large peak of glacial flour) within the MIS4 interval (Fig. 6) could be attributed to advances of the western Greenland ice margin comparable to those of MIS2 in scale. Unfortunately, 11 cm of sediments corresponding broadly to the 69–65.5 ka interval are missing, therefore preventing a precise interpretation of the glacial advance within that interval. Nonetheless, the hypothesis of a large advance of the ice margin on the western Greenland shelf at that time is in accordance with the lower relative sea-level (Cutler *et al.*, 2003; Fig. 6), low July insolation values (Laskar *et al.*, 2004; Fig. 6) and complementary evidence for the expansion of an ice shelf offshore south-western Greenland during MIS4 (Seidenkrantz *et al.*, 2010). From our study, we cannot ascertain an advance of the Uummannaq ice stream to the shelf edge during MIS4. However, lower PC1 values during MIS4, –5d/b compared with MIS2, together with facies dissimilarities, such as the amount of clay (Figs 2 and 6) or typical single domain magnetic grains (Simon, 2013), suggest a somewhat smaller ice stream expansion during MIS4, –5d/b, as well as a unique maximum extent to the shelf edge (i.e. MIS2) during the last glacial cycle. In this scenario of glacial margin advances, the central Baffin Bay sedimentary regime would have been in an 'ice proximal' mode (Fig. 7b) during MIS2 and to a lesser extent MIS4, –5d/b (and additional short intervals; Fig. 6) in contrast to periods when ice margins occupied an inner position over continental shelves. During these colder episodes, extensive shelf-edge-terminating ice streams probably feeding large ice shelf areas together with perennial sea ice cover contribute to reduce the marine surface area of Baffin Bay modifying oceanic circulation and sediment delivery into the bay (Fig. 7).

Comparison with numerical simulation and sea-level records

The LGM and pre-LGM Greenland ice stream dynamics reconstructed above is of particular importance with regard to ice sheet modeling experiments, suggesting that the maximum extent of the ice sheets in the circum-North Atlantic was comparable during both MIS5d/b and 2 (at least in surface extent, Ganopolski *et al.*, 2010). Our data point to major advances of the Greenland ice margin during MIS5d/b and MIS4. However, it is unlikely that they reached the MIS2 ice limits. Our findings are consistent with numerical simulations of ice sheet growth during the last glacial cycle (Marshall and Koutnik, 2006; Ganopolski *et al.*, 2010; Stokes *et al.*, 2012) associated with permanent ice-covered sea surface and a reduced oceanic circulation in Baffin Bay (Fig. 7; Hiscott *et al.*, 1989). By contrast, according to simulations, periods of Greenland ice stream retreat are associated with higher temperatures (shown by higher GISP2 $\delta^{18}O$ values, Fig. 6) and the probable advection of warm Atlantic waters into the bay (Srivastava *et al.*, 1987; Hiscott *et al.*, 1989; Jennings *et al.*, 2011) contributing to reduce the sea-ice/ice-shelf cover. During these 'warm' intervals, an increased cyclonic activity in Baffin Bay (Fig. 7a) would boost the winter snowfall on the Innuitian region (Marshall and Koutnik, 2006; Ganopolski *et al.*, 2010; Stokes *et al.*, 2012) contributing in turn to initiate northern fast-flowing ice streams. Such intervals correspond here to the 'long-duration' BBDC layers in core PC16, when intense ice streaming occurred in northern Baffin Bay (Simon, 2013) and, to a lesser extent, along the eastern Baffin Island (Fig. 6). Therefore, Greenland ice stream systems would have preferentially retreated during periods of increased advection of Atlantic water masses into Baffin Bay, thereby contributing to more unstable ice margin activities during the last glacial cycle. However, while our dataset exhibits considerable coherence with such a scenario, it cannot be said to strongly support the scenario either. Proxies for the advections of Atlantic water masses (e.g. Atlantic fauna, foraminiferal assemblage, sea surface temperature, sea ice cover) into Baffin Bay need to be tested to confirm this hypothesis. Such an incursion of Atlantic waters (via the West Greenland Current) has been recently documented during the last deglaciation by characteristic benthic foraminiferal assemblages in cores from the Greenland shelf (Sheldon, 2012).

Advances of the Uummannaq ice stream and sea level variations (Waelbroeck *et al.*, 2002; Cutler *et al.*, 2003) were apparently in phase during the last glacial cycle, which strongly support our interpretations (Fig. 6). Indeed, during the sea level lowerings, fast-flowing grounded ice streams advanced rapidly towards the (shallower) Greenland outer shelf, providing more Uummannaq sediments to central Baffin Bay.

Conclusions

The lithofacies and mineralogical properties of central Baffin Bay sediments spanning the last glacial cycle (i.e. 115 ka) are fairly consistent with recent ice-sheet numerical simulations (given their respective time resolution and uncertainty) for a rapid glacial inception and subsequent glacial growth and decay of the NE Laurentide, southern Innuitian and western Greenland Ice Sheets following the last interglacial. Development of the ice sheets and associated ice streams occurred as early as the MIS5d and MIS5b sub-stages. Maximum ice extent occurred during the early part of MIS4 (72–63 ka) and during an extended MIS2 (32–16 ka). Sediment signatures during MIS2 illustrate maximum extension of the Uummannaq ice stream to the shelf edge, whereas that of MIS4 sediments suggests a reduced Uummannaq ice stream expansion. The contribution of the eastern Baffin Island glaciers to the central Baffin Bay sedimentary budget is depicted by short-lived episodes of IRD and meltwater plumes in phase with NE Laurentide and southern Innuitian ice streaming episodes (i.e. BBDC events). Such coarse IRD intervals are seen as an 'ice-distal' pattern when the ice margins retreated behind their maximum extents, increasing the Baffin Bay marine surface area. By contrast, large increases of Uummannaq fine-grained sediments are interpreted as continuous expansions of the Greenland Ice Sheet during episodes of sea-level lowering. These episodes are represented by an 'ice-proximal' pattern wherein ice margins had advanced as far as the shelf edge, narrowing the Baffin Bay marine realm. We also propose that short-lived IRD events in Baffin Bay were mostly related to northern and eastern ice stream dynamics (i.e. NE Laurentide/Innuitian Ice Sheets and Baffin Island glaciers) due to climate forcings, while western Greenland sediments corresponded more to the extension and thickening of Greenland ice streams onto the outer shelf during glacial maxima. We suggest that these timing differences are explained by the distinct dynamics of the smaller Baffin Island glaciers and NE Laurentide/Innuitian ice streams, compared with that of the larger Greenland ice streams.

Supporting Information

Additional supporting information can be found in the online version of this article:

Fig. S1. Mineralogical estimates comparison between semi-quantitative XRD and quantitative XRD methods.
Fig. S2. Comparison of SedUnMix provenance wt% results for Uummannaq and eastern Baffin Island based on mineralogical assemblages measured by both XRD techniques.

Acknowledgements. We thank Michel Preda (UQAM) for assistance with XRD measurements, Pierre Francus and Arnaud de Coninck (INRS-ETE) for their help during the ITRAX core scanning. Special thanks are due to Martin Roy, Nicolas Van Nieuwenhove, David J. W. Piper and Colm Ó Cofaigh for constructive comments and reviews that significantly improved the manuscript. This study is part of the Canadian contribution to the Past4Future project. Support from MDEIE (Ministère du Développement Économique, de l'Innovation et de l'Exportation), NSERC (Natural Sciences and Engineering Research Council of Canada) through ship time and discovery grants to G.S. and C. H. M. FQRNT

(Fonds Québécois de la Recherche sur la Nature et les Technologies) and the CFI (Canadian Foundation for Innovation) is acknowledged.

Abbreviations. BBDC, Baffin Bay Detrital Carbonate; DOF, degrees-of-fit; GIS, Greenland Ice Sheet; IIS, Innuitian Ice Sheet; IRD, ice-rafted debris; LDC, Low Detrital Carbonate; LGM, Last Glacial Maximum; MIS, Marine Isotope Stage; ODP, Ocean Drilling Program; PCA, principal components analysis; RPI, relative paleointensity; XRD, X-ray diffraction; μXRF, micro X-ray fluorescence.

References

Aksu AE. 1981. Late Quaternary stratigraphy, paleoenvironmentology, and sedimentation history of Baffin Bafy and Davis Strait. PhD Thesis, Dalhousie University, Halifax, NS.

Aksu AE, Piper DJW. 1987. Late Quaternary sedimentation in Baffin Bay. *Canadian Journal of Earth Sciences* **24**: 1833–1846.

Alley RB, Andrews JT, Brigham-Grette J, *et al*. 2010. History of the Greenland Ice Sheet: paleoclimatic insights. *Quaternary Science Reviews* **29**: 1728–1756.

Andrews JT. 2000. Icebergs and iceberg rafted detritus (IRD) in the North Atlantic: facts and assumptions. *Journal of Oceanography* **13**: 100–108.

Andrews JT, Eberl DD. 2011. Surface (sea floor) and near-surface (box cores) sediment mineralogy in Baffin Bay as a key to sediment provenance and ice sheet variations. *Canadian Journal of Earth Sciences* **48**: 1307–1328.

Andrews JT, Eberl DD. 2012. Determination of sediment provenance by unmixing the mineralogy of source-area sediments: the ‘SedUnMix’ program. *Marine Geology* **291–294**: 24–33.

Andrews JT, Kirby M, Aksu AE, *et al*. 1998. Late Quaternary detrital carbonate (DC-) layers in Baffin Bay marine sediments (67°–74° N): correlation with Heinrich events in the North Atlantic? *Quaternary Science Reviews* **17**: 1125–1137.

Andrews JT, MacLean B. 2003. Hudson Strait ice streams: a review of stratigraphy, chronology and links with North Atlantic Heinrich events. *Boreas* **32**: 4–17.

Andrews JT, Jennings AE, Gibb OT, *et al*. 2013. Variations in the provenance of sediment from ice sheets surrounding Baffin Bay during MIS2 and 3 and export to the Labrador Shelf Sea: site HU2008029-0008 Davis Strait. *Journal of Quaternary Science*. [doi: 10.1002/jqs.2643]

Azetsu-Scott K, Clarke A, Falkner K. 2010. Calcium carbonate saturation states in the waters of the Canadian Arctic Archipelago and the Labrador Shelf Sea. *Journal of Geophysical Research* **115**: C11021.

Bigg GR, Wadley MR. 2001. The origin and flux of icebergs released into the Last Glacial Maximum northern hemisphere oceans: the impact of ice-sheet topography. *Journal of Quaternary Science* **16**: 565–573.

Bond GC, Lotti R. 1995. Iceberg discharges into the North Atlantic on millennial time scales during the Last Glaciation. *Science* **267**: 1005–1010.

Bond GC, Showers W, Elliot M, *et al*. 1999. The North Atlantic's 1–2 kyr climate rhythm: relation to Heinrich Events, Dansgaard/Oeschger cycle and the Little Ice Age. In *Mechanisms of Global Climate Change at Millennial Time Scales. Geophysical Monograph Series 112*, Clark P, Webb R, Keigwin L (eds). American Geophysical Union: Washington, DC; 35–58.

Briner JP, Miller GH, Davis PT, *et al*. 2003. Last Glacial Maximum ice sheet dynamics in Arctic Canada inferred from young erratics perched on ancient tors. *Quaternary Science Reviews* **22**: 437–444.

Briner JP, Miller GH, Davis PT, *et al*. 2006. Cosmogenic radionuclides from fiord landscapes support differential erosion by overriding ice sheets. *Geological Society of America Bulletin* **118**: 406–420.

Briner JP, Overeem I, Miller G, *et al*. 2007. The deglaciation of Clyde Inlet, northeastern Baffin Island, Arctic Canada. *Journal of Quaternary Science* **23**: 223–232.

Campbell DC, de Vernal A. 2009. CCGS Hudson Expedition 2008029: Marine geology and paleoceanography of Baffin Bay and adjacent areas, Nain, NL to Halifax, NS, August 28- September 23; Geological Survey of Canada, Open File 5989, 1 DVD.

Clark PU, Mix AC. 2002. Ice sheets and sea level of the Last Glacial Maximum. *Quaternary Science Reviews* **21**: 1–7.

Cutler KB, Edwards RL, Taylor FW, *et al*. 2003. Rapid sea-level fall and deep-ocean temperature change since the last interglacial period. *Earth and Planetary Science Letters* **206**, 253–271.

Davis JC. 2002. *Statistics and Data Analysis in Geology*, 3rd edn. Wiley: New York.

de Vernal A, Hillaire-Marcel C, Aksu AE, *et al*. 1987. Palynostratigraphy and chronostratigraphy of Baffin Bay deep sea cores: climatostratigraphic implications. *Palaeogeography, Palaeoclimatology, Palaeocology* **61**: 97–105.

Dowdeswell JA, Elverhøi A, Andrews JT, *et al*. 1999. Asynchronous deposition of ice-rafted layers in the Nordic seas and North Atlantic Ocean. *Nature* **400**: 348–351.

Dowdeswell JA, Hagen J, Björnsson H, *et al*. 1997. The mass balance of circum-Arctic glaciers and recent climate change. *Quaternary Research* **48**: 1–14.

Dowdeswell JA, Maslin MA, Andrews JT, *et al*. 1995. Iceberg production, debris rafting, and the extent and thickness of Heinrich layers (H-1, H-2) in North Atlantic sediments. *Geology* **23**: 301–304.

Dyke A. 2004. An outline of North American deglaciation with emphasis on central and northern Canada. *Developments in Quaternary Science* **2**: 373–424.

Dyke AS, Andrews JT, Clark PU, *et al*. 2002. The Laurentide and Innuitian Ice Sheets during the Last Glacial Maximum. *Quaternary Science Reviews* **21**: 9–31.

Eberl DD. 2003. User guide to RockJock: a program for determining quantitative mineralogy from X-ray diffraction data. United States Geological Survey, Open File Report 03-78, Washington, DC.

Eberl DD. 2004. Quantitative mineralogy of the Yukon River system: variations with reach and season, and determining sediment provenance. *American Mineralogist* **89**: 1784–1794.

England JH, Atkinson N, Bednarski J, *et al*. 2006. The Innuitian Ice Sheet: configuration, dynamics and chronology. *Quaternary Science Reviews* **25**: 689–703.

England JH, Furze MFA, Doupé JP. 2009. Revision of the NW Laurentide Ice Sheet: implications for paleoclimate, the northeast extremity of Beringia, and Arctic Ocean sedimentation. *Quaternary Science Reviews* **28**: 1573–1596.

Ehrhardt A, Gohl K, Neben S, *et al*. 2008. Davis strait and Ungava Fault Zone: first results from a recent geophysical survey. Eos Trans. AGU, 89(53), Fall Meet. Suppl., AGU Fall Meeting, San Francisco.

Funder S, Kjellerup K, Kjær K, *et al*. 2011. The Greenland Ice Sheet, the last 300,000 years: a review. In *Quaternary Glaciations, Extent and Chronology. Part IV. A Closer Look. Developments in Quaternary Science 16*. Elsevier: Amsterdam.

Ganopolski A, Calov R, Clausen M. 2010. Simulation of the last glacial cycle with a coupled climate ice-sheet model of intermediate complexity. *Climate of the Past* **6**: 229–244.

Harrison JC, St-Onge MR, Petrov O, *et al*. 2011. Geological map of the Arctic. Geological Survey of Canada, Map 2159A, scale 1:5000000.

Hemming SR. 2004. Heinrich events: massive Late Pleistocene detritus layers of the North Atlantic and their global climate imprint. *Reviews of Geophysics* **42**: RG1005.

Hillaire-Marcel C, de Vernal A, Aksu AE, *et al*. 1989. High-resolution isotopic and micropaleontological studies of Upper Pleistocene sediment at ODP site 645, Baffin Bay. In *Proceedings of the Ocean Drilling Program, Scientific Results leg 105-B*, Srivastava SP *et al*. Ocean Drilling Program: College Station, TX; 599–616.

Hiscott RN, Aksu AE, Nielsen OB. 1989. Provenance and dispersal patterns, Pliocene–Pleistocene section at site 645, Baffin Bay. In *Proceedings of the Ocean Drilling Program, Scientific Results Leg 105*, Srivastava SP *et al*. Ocean Drilling Program: College Station, TX; 31–52.

Holland DM, Thomas RH, De Young B, *et al*. 2008. Acceleration of Jakobshavn Isbrae triggered by warm subsurface ocean waters. *Nature Geoscience* **1**: 659–664.

Hulbe CL, MacAyeal DR, Denton GH, *et al.* 2004. Catastrophic ice shelf break up as the source of Heinrich event icebergs. *Paleoceanography* **19**: PA1004.

Jakobsson M, Mayer LA, Coakley B, *et al.* 2012. The International Bathymetric Chart of the Arctic Ocean (IBCAO), version 3.0. *Geophysical Research Letters* **39**: L12609. doi: 10.1029/2012GL052219

Jennings AE, Sheldon C, Cronin TM, *et al.* 2011. The Holocene history of Nares Strait: transition from glacial bay to Arctic-Atlantic throughflow. *Journal of Oceanography* **24**: 26–41.

Laskar JP, Robutel F, Joutel F, *et al.* 2004. A long term numerical solution for the insolation quantities of the Earth. *Astronomy and Astrophysics* **428**: 261–285.

Li G, Piper DJW, Campbell DC. 2011. The Quaternary Lancaster Sound trough-mouth fan, NW Baffin Bay. *Journal of Quaternary Science* **26**: 511–522.

MacAyeal DR. 1993. Binge-purge oscillations of the Laurentide Ice Sheet as a cause of the North Atlantic's Heinrich events. *Paleoceanography* **8**: 775–784.

MacLean B, Blasco S, Bennett R, *et al.* 2010. Ice keel seabed features in marine channels of the central Canadian Arctic Archipelago: evidence for former ice streams and iceberg scouring. *Quaternary Science Reviews* **29**: 2280–2301.

Maclean B, Williams GL, Srivastava SP. 1990. Geology of Baffin Bay and Davis Strait. In *Geology of Canada No.2: Geology of the continental margin of eastern Canada*, Keen MJ, Williams GL (eds). Geological Survey of Canada: 293–348.

Marcott SA, Clark PU, Padman L, *et al.* 2011. Ice-shelf collapse from subsurface warming as a trigger for Heinrich events. *Proceedings of the National Academy of Sciences of the USA* **108**: 13415–13419.

Marshall SJ, Koutnik MR. 2006. Ice sheet action versus reaction: distinguishing between Heinrich events and Dansgaard-Oeschger cycles in the North Atlantic. *Paleoceanography* **21**: PA2021.

Ó Cofaigh C, Andrews JT, Jennings AE, *et al.* 2012. Glacimarine lithofacies, provenance and depositional processes on a West Greenland trough-mouth fan. *Journal of Quaternary Science* doi: 10.1002/jqs.2569

Ó Cofaigh C, Dowdeswell JA, Jennings AE, *et al.* 2013. An extensive and dynamic ice sheet on the west Greenalnd shelf during the last glacial cycle. *Geology* **41**: 219–222.

Parnell J, Bowden S, Andrews JT, *et al.* 2007. Biomarker determination as a provenance tool for detrital carbonate events (Heinrich events?): fingerprinting Quaternary glacial sources into Baffin Bay. *Earth and Planetary Science Letters* **257**: 71–82.

Petersen SV, Schrag DP, Clark PU. 2013. A new mechanism for Dansgaard-Oeschger cycles. *Paleoceanography* **28**: 1–7. [doi: 10.1029/2012PA002364]

Rignot E, Mouginot J. 2012. Ice flow in Greenland for the International Polar Year 2008. *Geophysical Research Letters* **39**: L11501.

Seidenkrantz MS, Kuijpers A, Aagaard-Sørensen S, *et al.* 2010. Glacial ocean circulation and shelf edge glaciation offshore SW Greenland during the past 75.000 years. *Geophysical Research Abstract*, vol. **12**: EGU2010-4721.

Sheldon C. 2012. The deglacial History and Paleoceanography of the Uummannaq System, West Greenland. MSc thesis, University of Colorado.

Simon Q. 2013. Propriétés magnétiques, minéralogiques et sédimentologique des sédiments profond de la baie de Baffin: chronologie et dynamique des glaciers ouest groenlandais, innuitiens et laurentidiens au cours de la dernière glaciation. *PhD Thesis*, Université du Québec à Montreal.

Simon Q, St-Onge G, Hillaire-Marcel C. 2012. Late Quaternary chronostratigraphic framework of deep Baffin Bay glaciomarine sediments from high-resolution paleomagnetic data. *Geochemistry, Geophysics, Geosystems* **13**: Q0AO03. doi: 10.1029/2012GC004272

Srivastava SP. 1989. *Proceedings of the Ocean Drilling Program, Scientific Results. Baffin, Bay and Labrador Sea. Leg 105, Sites 645–647*. Ocean Drilling Program: College Station, TX.

Srivastava SP, Arthur M, Clement B. 1987. Introduction. *Proceedings of the Ocean Drilling Program, Scientific Results Leg 105*, Srivastava SP, Arthur M, Clement B (eds). Ocean Drilling Program: College Station, TX; 5–20.

St-Onge G, Mulder T, Francus P, *et al.* 2007. Continuous physical properties of cored marine sediments. In *Developments in Marine Geology. Proxies in Late Cenozoic Paleoceanography*, vol. 1 Hillaire-Marcel C, de Vernal A (eds). Elsevier: Amsterdam; 63–98.

Stokes CR, Clark CD. 2001. Palaeo-ice streams. *Quaternary Science Reviews* **20**: 1437–1457.

Stokes CR, Tarasov L. 2010. Ice streaming in the Laurentide Ice Sheet: a first comparison between data-calibrated numerical model output and geological evidence. *Geophysical Research Letters* **37**: L01501.

Stokes CR, Tarasov L, Dyke AS. 2012. Dynamics of the North American Ice Sheet Complex during its inception and build-up to the Last Glacial Maximum. *Quaternary Science Reviews* **50**: 86–104.

Tang C, Ross C, Yao T, *et al.* 2004. The circulation, water masses and sea-ice of Baffin Bay. *Progress in Oceanography* **63**: 183–228.

Thorez J. 2003. L'argile, minéral pluriel. *Bulletin de la Société Royale des Sciences de Liège* **72**: 19–70.

Waelbroeck C, Labeyrie L, Michel E, *et al.* 2002. Sea-level and deep water temperature changes derived from benthic foraminifera isotopic records. *Quaternary Science Reviews* **21**: 295–305.

Weidick A, Bennike O. 2007. Quaternary glaciation history and glaciology of Jakobshavn Isbræ and the Disko Bugt region, West Greenland: a review. *Geological Survey of Denmark and Greenland Bulletin* **14**.

Young NE, Briner JP, Rood DR, *et al.* 2012. Glacier extent during the Younger Dryas and 8.2-ka event on Baffin Island, Arctic Canada. *Science* **337**: 1330–1333.

